Diabetic Complications Consortium

Application Title: Transformative Tools for Imaging Tissue Ultrastructure in Diabetic Kidney Disease

Principal Investigator: Prof. Joshua C. Vaughan

1. Project Accomplishments:

We developed and applied procedures using advanced fluorescence and electron microscopy techniques for the study of mouse and human kidney tissue. These include the following highlights.

- We developed techniques for isotropic expansion of fresh mouse and human kidney tissue to enable high-resolution study of kidney tissue using fluorescent microscopy. This enables researchers to retain all the benefits of fluorescence (routine volumetric imaging, labeling of specific molecules, and multichannel imaging) together with spatial resolution of ~65 nm. This work was published along with a detailed step-by-step protocol to enable other researchers to utilize our methodology (Chozinski et al. 2018). This methodology was utilized as part of ongoing collaborations in two additional studies (Kaverina et al. 2019 and Glaser et al. 2019).
- We extended our expansion techniques to FFPE (formalin-fixed, paraffin-embedded) mouse and human kidney tissue. We pursued this in parallel with the development of procedures for small-molecule stains that are fluorescent analogs of classic histology stains and use only commercially available reagents. These stains enable routine volumetric multichannel imaging in combination with other fluorescence stains such as immunostains or in situ hybridization stains of nucleic acids. This work is currently in review.
- We have developed methodologies to obtain volumetric data from human diabetic and control kidney biopsies using transmission electron microscopy (TEM) and serial block-face scanning electron microscopy (SBF-SEM). These results provide unprecedented high-resolution views of human kidney tissues and have revealed a wealth of details. For instance, a careful analysis of these results showed that diabetic nephropathy modulates the architecture of sub-podocyte spaces and exit pores relative to control tissues.

2. Specific Aims:

Specific Aim 1. Develop protocols to study fresh kidney tissue by expansion microscopy (ExM) in diabetic and control human and mice.

Results: We successfully developed and validated protocols for expansion microscopy (ExM) on fresh healthy mouse and human kidney tissue that enabled high-resolution (~70nm) optical microscopy studies at four-fold higher resolution than traditional optical microscopy techniques. The results were published in 2018 in an open-access article whose supplementary information includes a detailed step-by-step protocol for how to reproduce the procedures. This will enable researchers to use standard, widely available optical microscopes to study the nanoscale distributions of proteins and other molecules for the analysis of mouse and human kidney tissue.

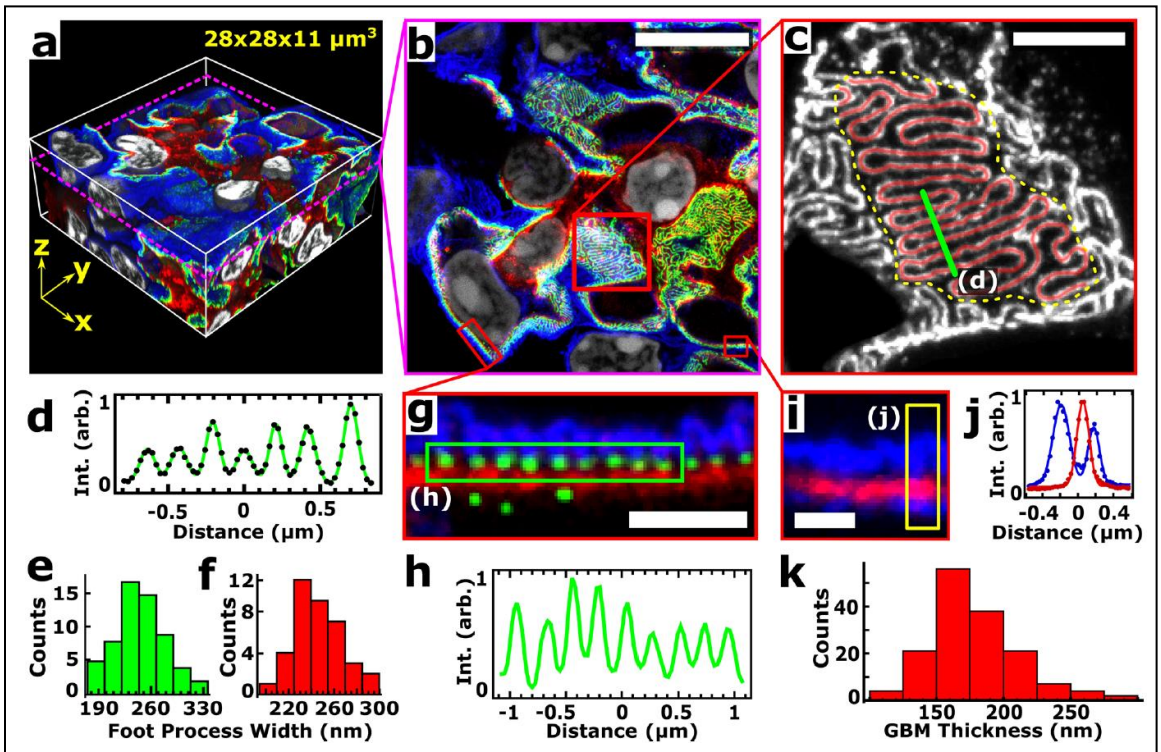

Figure 1. Expansion microscopy on freshly-fixed mouse kidney tissue immunostained for podocin (green), agrin (red), podocalyxin (blue), and stained for DNA (white). (**b**) A single plane from volumetric data in (a). (**c**) Zoomed-in view of podocin channel and (**e-f**) analysis of foot process width. (**g**) Zoomed-in view of boxed region in (b) and (**h**) cross-sectional profile of glomerular filtration barrier. (**i**) Zoomed-in view of the podocalyxin (blue) and agrin (red) channels from the boxed region in (b). (**k**) Histogram of glomerular basement membrane thickness. All distances and scale bars are in pre-expansion units. Scale bars, 8 μm (**b**), 2 μm (**c**), 1 μm (**g**), and 500 nm (**i**). See Chozinski et al. Sci. Rep., 2018 for more details and the supplementary online materials for a video animation of this data set.

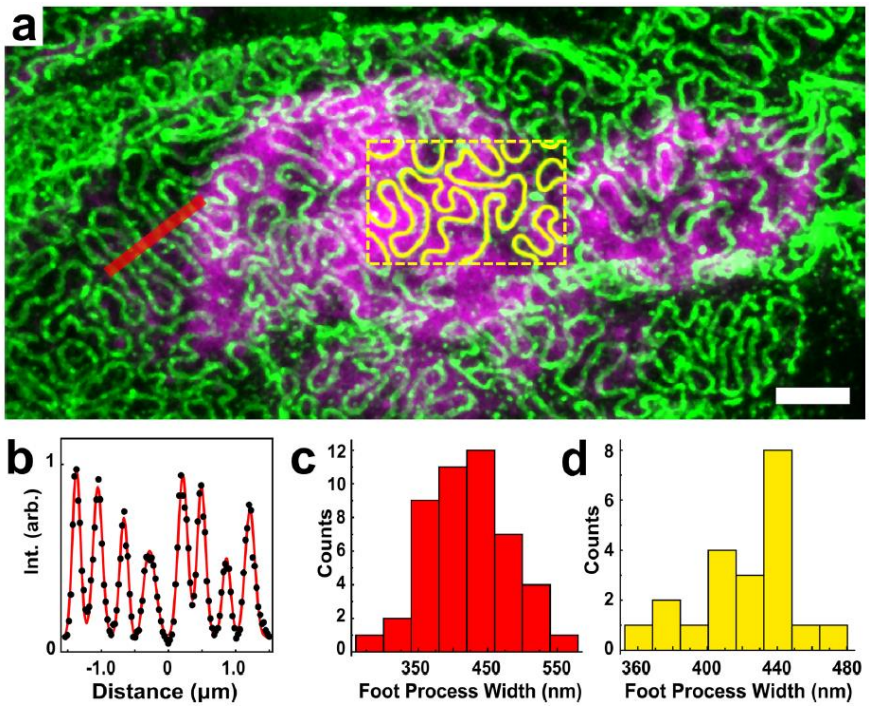

Figure 2. ExM image of (**a**) expanded human kidney immunostained for podocin (green) with nuclei stained by Hoechst (magenta). (**b**) Cross-sectional profile and anslysis of foot process widths. All distances and scale bars are in pre-expansion units. Scale bar, 2 μm (**a**). See Chozinski et al. Sci. Rep., 2018 for more details.

We faced difficulty with the development of a protocol for expansion of diabetic mouse kidney tissue since the tissue tended to be quite fibrotic and resisted our procedures to homogenize (digest) the tissue to render it compliant with the hydrogel expansion. We continue to work on developing procedures that are able to homogenize tough tissues.

Specific Aim 2. Develop protocols to study formalin fixed paraffin embedded kidney tissue by ExM in diabetic and control human and mice.

Results: We successfully developed procedures that enable the expansion of formalin-fixed paraffin-embedded (FFPE) mouse and human kidney tissue (**Figure 3**). Related to this effort, we also developed a three-color fluorescent stain using commercial small-molecules stains that is the fluorescent analog of the H&E stain together with PAS stain (**Figure 4**). The stains are able to efficiently reveal key landmarks in cells and tissues under different fixation or sample processing conditions for both expanded tissues (i.e., high resolution studies) and for cleared tissues (for imaging of thick, intact specimens).

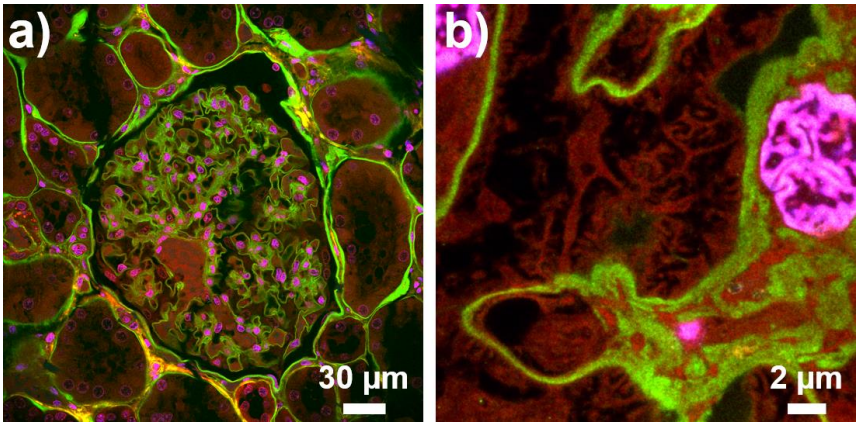

Figure 3. ExM images of expanded FFPE human kidney tissue at (**a**) low magnification and (**b**) high magnification. All scale bars are in pre-expansion units. See Figure 4, below, for more detail on stains.

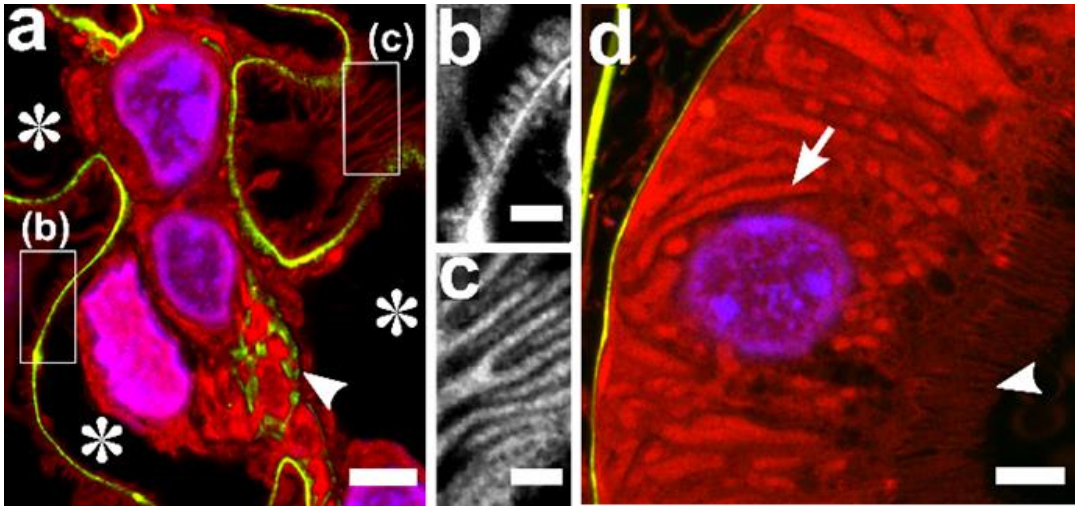

Figure 4. ExM image of expanded mouse kidney stained for nuclei (blue) with Hoechst, stained for protein (red) with amine-reactive fluorophores, and stained for carbohydrates (green) with an oxidized . (**a**) Region of a glomerulus. (**b-c**) Zoom-in view of boxed regions in panel (a).

Specific Aim 3. Correlative ExM/EM studies in diabetic and control human and mice.

Results: As a critical step for correlative ExM/EM. We have developed methodologies to obtain volumetric data from human diabetic and control kidney biopsies using transmission electron microscopy (TEM) and serial block-face scanning electron microscopy (SBF-SEM). Protocols were developed to identify and segment subpodocyte space (SPS), interpodocyte space (IPS), peripheral urinary space (PUS) and to measure the structural properties of those spaces on TEM images (**Figure 5**). Comparison of glomeruli from 5 macroalbuminuric, 3 microalbuminuric and 3 normoalbuminuric Pima Indians with type 2 diabetes (T2D) and 5 age-matched normal controls showed classical changes of diabetic nephropathy. In parallel with increased glomerular volume, the volume and the glomerular basement membrane (GBM) surface exposed to each of the

urinary space compartments including SPS, IPS and PUS were increased in diabetic nephropathy (DN), surface density of SPS and IPS were reduced in DN subjects and this reduction was more prominent for SPS (over 2 fold) (**Figure 5**). Moreover, in DN patients, fraction of GBM surface which is exposed to SPS was reduced and, in contrast, fraction of GBM exposed to IPS was increased (**Figure 6**). These findings suggest that structural properties of these spaces are differentially regulated in DN. In addition, since SPS induces the most resistance against the filtration flow, reduced fraction of GBM exposed to SPS may be a compensatory mechanism against GFR loss in DN. Validation of extrapolation of the two-dimensional approach (TEM) to volumetric data (SBF-SEM and ExM) was performed as follows. SPS, IPS and PUS were identified on z-stack of images. SPS/IPS exit pores were identified and segmented. Diameter of SPS/IPS exit pores on each profile was measured separately. A random measurement in each set was selected as presumed measurement on TEM. The average of all measurements on volumetric sets was 2270±1131 pixels and the average of all random (two-dimensional) measurements was 2133±1365 pixels (6% different and not statistically significant).

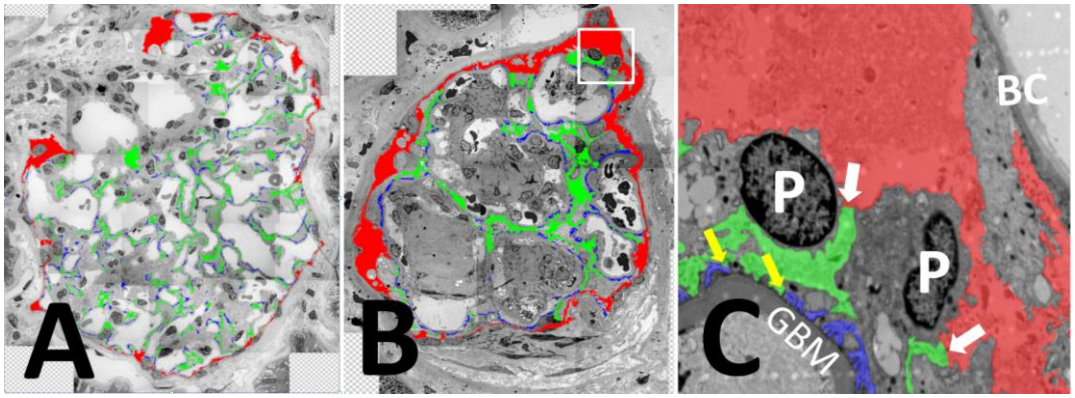

Figure 5. Segmentation of SPS (blue), IPS (green) and PUS (red) in human normal control **(A)** and diabetic nephropathy **(B)**. **(C)** is a magnified view of the white box in (B) showing glomerular basement membrane (GBM), podocytes (P), Bowman's capsule (BC), exit pores connecting SPS to IPS (yellow arrows) and exit pores connecting IPS to PUS (white arrows).

There was a strong negative correlation between total surface area of IPS [S(IPS/glom)] and Nv(PC/glom) (r=-0.93, p=0.02), which although likely an over-fit regression due to limited number of cases, it suggests that podocyte loss may be associated with increased bridging of podocytes between adjacent capillary loops and thereby increasing IPS. Our preliminary data suggest that with DN progression, the length of the SPS exit pores (SEP) increases which may be related to podocyte hypertrophy. The data also indicates that there is a trend towards increase in average area of SEPs along with progression of DN and proteinuria. The observed changes in dimensional properties of exit pores (area and length) have opposite effects on the final resistance created in urinary spaces against filtration. It is plausible that increase in length will result in more resistant out-flow and in contrary, larger SEP areas will provide less resistant pathways. Both of these phenomena may be related to podocyte loss and hypertrophy that occur during natural history of the disease. Incorporating all of the quantifiable in-flow and out-flow properties of urinary spaces and other glomerular ultrastructural changes into our model and validating the results using 3-D reconstruction rendering methods in different

diseased and normal conditions, would enable us to accurately predict and measure the net effect of these changes on resistance to fluid-flow and single-nephron GFR.

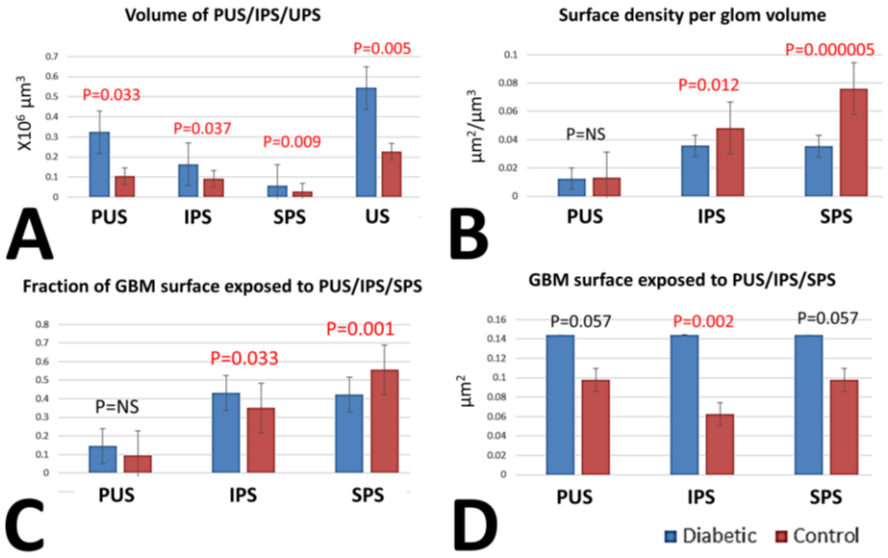

Figure 6. Comparison of various properties of SPS/IPS and PUS in control (red) and diabetic nephropathy (blue) subjects

We have also prepared 3D models of SPD and IPS with exit pores connecting the two spaces using both ExM and SBF-SEM. The results confirm that ExM is a powerful tool to obtain volumetric data about SPS, especially since sampling larger spaces is more feasible by ExM compared with SBF-SEM (**Figure 7**).

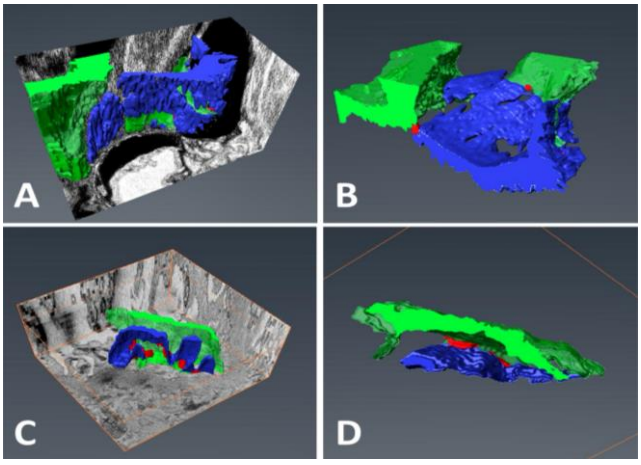

Figure 7. Three-dimensional modeling of SPS (blue), IPS (green) and the exit pores connecting SPS to IPS (red) in mouse kidney using ExM (A and B) and human kidney using SBF-SEM (C and D). (A and C) show the 3D model within the context of the background tissue and (B and D) show the models without the background.

3. Publications:

T.J. Chozinski, C. Mao, A.R. Halpern, J.W. Pippin, S.J. Shankland, C.E. Alpers, B. Najafian, J.C. Vaughan, "Volumetric, Nanoscale Optical Imaging of Mouse and Human Kidney via Expansion Microscopy." *Sci. Rep.* 8 (1), No. 10396 (2018).

A.K. Glaser, N.P. Reder, Y. Chen, C. Yin, P. Wei, S. Kang, L.A. Barner, W. Xie, E.F. McCarty, C. Mao, A.R. Halpern, C. Stoltzfus, M.Y. Gerner, P.R. Nicovich, J.C. Vaughan, L.D. True, J.T.C. Liu "Multi-immersion open-top light-sheet microscope for high-throughput imaging of cleared tissues." *Nat. Commun.* 10, 2781-2789 (2019).

N.V. Kaverina, D.G. Eng, B.S. Freedman, N.J. Kutz, T.J. Chozinski, J.C. Vaughan, J.H. Miner, J.W. Pippin, S.J. Shankland "Dual Lineage Tracing Shows That Glomerular Parietal Epithelial Cells Can Transdifferentiate Towards The Adult Podocyte Fate" *Kidney Int.* 96 (3), 596-611 (2019).